sustainability

MDPI

Concept Paper

TopCycle: A Novel High Performance and Fuel Flexible Gas Turbine Cycle

Simeon Dybe [1,*], Michael Bartlett [2], Jens Pålsson [2] and Panagiotis Stathopoulos [3]

[1] Fluid Dynamics, Technische Universität Berlin, 10623 Berlin, Germany
[2] Phoenix BioPower AB, Drottning Kristinas väg 18, 114 24 Stockholm, Sweden; michael.bartlett@phoenixbiopower.com (M.B.); jens.palsson@phoenixbiopower.com (J.P.)
[3] Unsteady Thermodynamics in Gas Turbine Processes, Technische Universität Berlin, 10623 Berlin, Germany; stathopoulos@tu-berlin.de
* Correspondence: dybe@tu-berlin.de

Abstract: High pressure humidified cycles can combine high operational flexibility and high thermal efficiency. The current work introduces such a cycle, namely TopCycle, which provides the necessary combustion infrastructure to operate on a wide fuel variety in a steam-rich atmosphere. The cycle configuration is presented in detail, and its operation is exemplified on the basis of simulation results. Operation at design condition results in electric efficiencies higher than 50% (lower heating value (LHV)) and power densities higher than 2100 kW/kg$_{air}$ (referred to intake air flow). A sensitivity analysis identifies the cycle performance as a function of representative parameters, which provide the basis for future operation and design improvements. As for any gas turbine cycle, TopCycle's electric efficiency can be effectively improved by increasing the turbine inlet temperature, optimizing the economizer heat recovery, as well as elevating the working pressure. Finally, TopCycle's performance is compared to a state-of-the-art combined cycle (CC) at equivalent operation parameters. The TopCycle operates at an elevated electric efficiency and considerably higher power density, which can be transferred into smaller plant footprint and dimensions and thus lower investment costs at equal power output in comparison to a CC.

Keywords: TopCycle; wet cycle; Phoenix BioPower; cycle analysis; power and heat generation; BTC cycle

Citation: Dybe, S.; Bartlett, M.; Pålsson, J.; Stathopoulos, P. TopCycle: A Novel High Performance and Fuel Flexible Gas Turbine Cycle. *Sustainability* **2021**, *13*, 651. https://doi.org/10.3390/su13020651

Received: 9 December 2020
Accepted: 22 December 2020
Published: 12 January 2021

1. Introduction

Restructuring the energy sector towards renewable and low emission electricity generation is an imperative aim of the global community if climate change is to be stopped. Gas turbines are a very flexible power and heat generation technology that could become a major supporting technology in this transition. Although simple-cycle gas turbines can be operated in a flexible way, they have a relatively low thermal efficiency. On the other hand, combined cycle plants (CC) utilize the exhaust heat of gas turbines to generate more power through an additional steam bottoming cycle. Although this leads to a higher thermal efficiency, these systems suffer from limited operational flexibility [1], mostly due to the high pressure components of the additional steam cycle.

Wet gas turbine cycles offer a way to combine the low capital costs and fast ramp times of a simple cycle gas turbine with the high electrical efficiency of the CC [2]. Especially in the range of medium sized plants, up to 100 MW, wet cycle gas turbines can achieve thermal efficiencies comparable to combined cycle power plants at considerably higher power density and operational flexibility. Already today, several hundred units of such cycles have found commercial application also as a retrofitting option for existing gas turbines, i.e., the Cheng cycle or the steam injected gas turbine (STIG) cycle [1]. Further, Traverso et al. [3] concluded that humidified cycles are good alternatives to combined cycles at relatively low power outputs, where the bottoming cycle of combined cycles

becomes thermodynamically less efficient. The results of their thermoeconomic analysis ascribe humidified cycles a great economic potential in the range of 50 MW.

The effect of steam injection on the cycle performance was reported in many theoretical and experimental studies. In their work, Gasparovic and Hellemans [4] found that the increase of thermal efficiency in a steam injected gas turbine (STIG) cycle is comparable to that resulting from a rise in turbine inlet temperature (TIT) by 100 °C in a simple gas turbine cycle. They also mentioned that the gain in specific power corresponds to an even higher equivalent increase in firing temperature of 140 °C. Further, Parente et al. [5,6] provided a model that covers both a thermodynamic and thermoeconomic analysis, for a micro HAT (humid air turbine) cycle and reported an efficiency and specific work increase over an equivalent micro gas turbine (mGT) cycle by 5% and 50%, respectively. Finally, Stathopoulos et al. [7] presented similar results in their study, which compared commercial gas turbines adapted to steam injection to their dry alternatives. In all cases, the thermal efficiency and power output were higher with steam injection than in the dry cycle. Furthermore, the efficiency rises with increasing pressure ratios, which favors pressure ratios over 40 and TIT over 1600 °C. In a similar context, simulations by Bartlett and Westermark [8] on evaporative cycles came to the result that these cycles have a higher thermal efficiency than combined cycles for cycle pressure ratios above 40 and the same firing temperature. They also found that combined cycles perform better for pressure ratios between 20 and 40. Moreover, steam injection in the combustion chamber can be used to facilitate pure hydrogen combustion at ultra low emissions, without making considerable changes in the combustion system architecture [9].

Bartlett [10] studied several wet combustion gas turbine cycles as part of combined heat and power applications (CHP) and compared their energetic efficiency to that of an equivalent combined cycle. Wet cycles can perform at over 30% lower investment costs and over 10% lower cost of electricity levels when compared to a CC. Parente et al. [5,6] analyzed the effect of humidification on the operational flexibility of the system, when operated as CHP unit in a district heating application. The topic of operational flexibility and its impact on the thermo-economical performance of wet CHP-micro gas turbines was also the topic of the works from Stathopoulos et al. [11,12], De Paepe et al. [13], and Carrero et al. [14] for the STIG-mGT and the HAT-mGT cycles, respectively. They all concluded that apart from the increase in electrical efficiency, the respective wet cycles increase the equivalent full load operational hours of the CHP systems and improve their economic performance.

The current work is in effect an extension of the work performed by Bartlett and Westermark [15,16], by presenting a new concept for a high pressure wet cycle, TopCycle. TopCycle represents a strong and promising option in the category of modern small and medium sized power plants and offers highly efficient power and heat generation at plant sizes, which cannot be feasibly covered with CC. Moreover, TopCycle provides the necessary combustion infrastructure to operate on a wide fuel variety in a steam-rich atmosphere, where the fuel spectrum extends from conventional fuel sources like natural gas to combustibles from renewable sources such as bio-syngas and hydrogen. Thus, it actively supports the transition towards a renewable and low emission energy generation and makes this cycle concept a perfect link between the established electricity production methods and the energy market of the future.

The work, which is focused on a mid-sized CHP system, starts with a presentation of the cycle concept and topology, followed by methods to simulate the cycle, the logic behind the parameter variation studies, and finally, a presentation of the results. TopCycle and a state-of-the-art combined cycle power plant are then compared for similar plant output and operation parameters.

2. TopCycle Description

TopCycle as shown in Figure 1 is an extended version of a wet cycle, which is equipped with the required technology to run on a variety of fuels such as synthesis gas from biomass

or (renewable) natural gas. This work presents the natural gas version of TopCycle as patented by Westermark and Hansson [17]. Basically, the cycle consists of a gas turbine section featuring compression, combustion, and expansion and a system for heat extraction comprising recuperation, as well as heat extraction for cycle-external usage. Water that is re-introduced into the cycle for humidification and cooling purposes fully stems from the exhaust gas condensation.

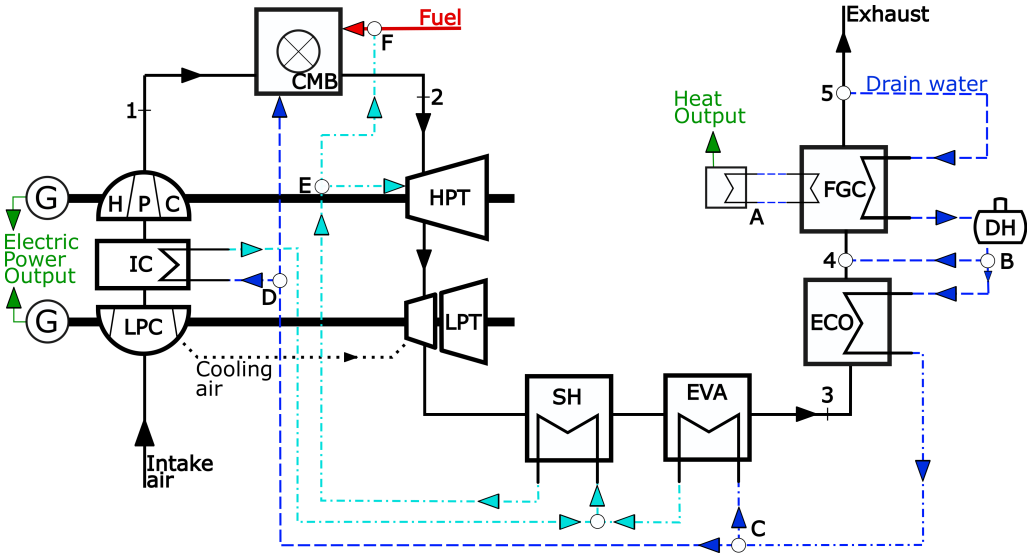

Figure 1. Schematic of TopCycle. Liquid water streams are indicated as blue dotted lines and steam as turquoise dashed/dotted lines. G, generator; HPC, high pressure compressor; IC, intercooling; LPC, low pressure compressor; CMB, combustion chamber; HPT, high pressure turbine; LPT, low pressure turbine; SH, superheater; EVA, evaporator; FGC, flue gas condenser; ECO, economizer; DH, district heating.

Air at ambient condition is pressurized in the low pressure compressor (LPC), and compression heat is extracted by an intercooler (IC) for steam generation. The working pressure (Point 1) is achieved by further compression in the high pressure compressor (HPC).

Air, steam, fuel, and water at working pressure are fed to the combustion chamber (CMB) and burned close to stoichiometric.

The hot flue gas (Point 2) is expanded in two steps. First, it enters the high pressure turbine (HPT), which is simulated as one stage with its stator and rotor cooled with steam from the steam cycle. The cooling mass flow is computed using a cooling algorithm presented in Section 3.1. The HPT is located on the same shaft as the HPC and a generator (G), the top spool.

The bottom spool (LPC, low pressure turbine (LPT), and generator) is powered by the LPT. Here, the flue gas is expanded to near ambient pressure (Point 3). The LPT is modeled with two stages, the first one of which is cooled by pressurized air provided by the LPC, and the second uncooled.

After expansion, the flue gas is fed to the heat recovery steam generator (HRSG), which typically consists of an economizer (ECO), an evaporator (EVA), and a superheater (SH). Finally, a flue gas condenser (FGC) system uses low temperature heat and releases the exhaust gas at a temperature considerably lower than the dew point of water at atmospheric pressure. Here (Point A), cooling water in an external loop is provided to the FGC, where it is heated close to the dew point temperature of the flue gas. This so extracted heat can serve in cycle-external usage, e.g., in district heating (DH) applications.

In the FGC, much of the flue gas' steam content is condensed before releasing exhaust gas to the stack (Point 5). The water flow required for cycle internal usage can be fully sustained from the condensation. At Point B, enough water is injected upstream of the FGC to fully saturate the gas stream to achieve the maximum dew temperature (Point 4). The

remaining water flow passes through a condensate cleaning system to remove impurities and a deaerator tank (DA) to remove dissolved gases. Condensate water of feed water quality is then re-injected at several points in the cycle.

Water is preheated in the economizer and further directed to the evaporator (Point C), the IC (Point D), and the combustor. Steam is raised in both the EVA and the IC, while the rest of the water is directly evaporated in the combustor. Steam from the boiler sections (EVA and IC) is superheated in the SH. Subsequently, the required amount for turbine cooling is extracted at Point E. A large part of the superheated steam is injected into the combustor. Steam addition and water vaporizing in the CMB aim to increase the power density.

3. Model Description

The commercial software Ebsilon Professional by Steag was used for the simulation [18]. The properties of steam and water are based on the IAPWS-IF97data [19]. The TopCycle's basic model assumptions can be found in Table 1.

TopCycle can serve as the supplier in district heating systems. Its FGC recovers low temperature exhaust heat to raise water temperature from 40 °C to 3 °C below the water dew point of the flue gas at over 80 °C. Reference [20] gave average supply and return temperatures for Swedish DH systems of 86 °C and 47 °C and the Berlin DH supplier of 80-135 °C and up to 56 °C [21], respectively, which puts FGC performance within a realistic DH operation temperature range.

The fuel is natural gas with a composition as in Table 1. The assumptions for compressor and turbine isentropic efficiency and pressure losses are in the range of state-of-the-art turbomachinery. Here, assumed values for the pressure ratio of the LPC and HPC, as well as for the TIT lie within the typical range of the respective engine power class.

Table 1. Thermodynamic layout data. HRSG, heat recovery steam generator.

TopCycle		
Fuel		Natural Gas
Fuel LHV	(MJ/kg)	46.48
Ambient pressure	(bar)	1.013
Ambient temperature	(°C)	15
Combustor pressure loss	(bar)	-
Air ratio λ		1.1
Turbine inlet temperature	(°C)	1350
Turbine inlet pressure	(bar)	43.7
LPT/HPT turbine isentropic efficiency [22,23]	(%)	91/87
LPC/HPC isentropic efficiency [22,23]	(%)	87/84
LPC/HPC pressure ratio		15/3.34
Pump isentropic efficiency [22]	(%)	70
HRSG pressure loss hot side	(%) of p_{in}	2.8
HRSG pressure loss cold side	(%) of p_{in}	4.2
HRSG pinch point	(K)	8
SH degree of superheating	(°C)	50
Generator efficiency	(%)	97.4
FGC pinch point	(K)	3
Return temperature FGC	(°C)	40
Fuel composition		
Methane	(%)	86.2
Ethane	(%)	8.56
Carbon dioxide	(%)	1.91
Propane	(%)	1.89
Nitrogen, n-butane, n-pentane, n-hexane		Rest

3.1. Turbine Cooling Flows

The turbine cooling model is based on the method presented by Horlock [24]. The method computes the cooling mass flows required to keep the blade temperatures below a specified value and is executed in every loop of the simulation.

A cooled turbine stage is separated into three individual elements, which represent the stator cooling, the expander, and the rotor cooling. In this case, the expander is modeled by the standard gas turbine component in Ebsilon. The rotor and stator cooling are realized via injection of the respective cooling medium (water or air) into the gas stream (open loop) in the model, where the stator coolant is fed to the gas flow upstream of the expander and the rotor coolant flow downstream, respectively. Pressure drops during the mixing process are neglected, and blade temperature is assumed uniform. The structure of a cooled turbine stage is shown in Figure 2.

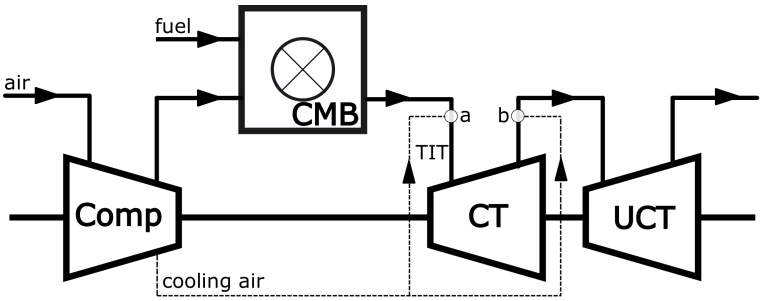

Figure 2. Schematic of an air-cooled turbine. TIT, turbine inlet temperature; CT, cooled turbine stage; UCT, uncooled turbine stage.

The calculation method of the required coolant flow assumes a constant external Stanton number. The ratio Ψ of the cooling mass flow rate with respect to the gas mass flow rate entering the turbine:

$$\psi = \frac{\dot{m}_{cool,in}}{\dot{m}_{gas,in}} \quad (1)$$

is computed as a function of the temperatures of the coolant, $T_{cool,in}$, and the gas, $T_{gas,in}$. Further, the applied cooling method, i.e., external film cooling, is represented by parameters describing the method's cooling system technology level and its effectiveness. Finally, the algorithm computes the sufficient amount of cooling mass stream with the goal of achieving an acceptable blade temperature, T_{blade}. Originally, the method was derived for air cooling, whereas for this work, both steam and air are deployed. The respective parameters to estimate Ψ applied in this model are presented in Table 2 (similar numbers can be found in Horlock [24]).

Table 2. Cooling model parameters.

Parameter	Symbol	Value
Level of technology constant	C	0.045
Film cooling effectiveness	ϵ_F	0.4
Cooling efficiency	η_{cool}	0.7
Blade temperature HPT	T_{blade} (°C)	950

3.2. Key Cycle Parameters

The cycle's net efficiency is the ratio of the useful power, i.e., the difference between the generator power and cycle internal power losses as compression and friction, versus the energy in the fuel.

$$\eta_{cycle} = \frac{\sum P_{production} - \sum P_{losses}}{\dot{m}_{fuel} \cdot LHV} \quad (2)$$

The total efficiency of the system includes the heat extracted in the FGC for external usage as gain, which can be utilized, e.g., in district heating applications.

$$\eta_{total} = \frac{\sum P_{production} - \sum P_{losses} + Q_{DH}}{\dot{m}_{fuel} \cdot LHV} \quad (3)$$

The specific power w is defined as the turbine power output normalized by the compressor intake mass flow.

$$w = \frac{P_{HPT} + P_{LPT}}{\dot{m}_{LPC,in}} \quad (4)$$

The excess air ratio λ of the combustion is defined based on the condition present in the combustion chamber (CMB) according to:

$$\lambda = \left. \frac{\dot{m}_{air,actual}}{\dot{m}_{air,stoichiometric}} \right|_{CMB} \quad (5)$$

3.3. Simulation Structure

In the simulation, air flow is kept constant, and all other streams are computed relative to that. Fuel and air flows are supplied at ambient pressure and temperature at standard reference conditions (ISO). In the sensitivity analysis, presented in Section 4, the influence on the cycle's performance is investigated for the following parameters.

- steam mass flow raised in the IC, $\dot{m}_{IC}$—two modes of operation:
  - $\dot{m}_{IC}$ is specified by an input value
  - IC raises the maximum $\dot{m}_{IC}$ based on the available heat
- steam mass flow raised in the EVA, $\dot{m}_{EVA}$—two modes of operation:
  - $\dot{m}_{EVA}$ is specified by an input value
  - EVA raises the maximum $\dot{m}_{EVA}$ based on the available heat
- water mass flow injected into the CMB, $\dot{m}_{liq}$—two modes of operation:
  - $\dot{m}_{liq}$ is specified by an input value
  - $\dot{m}_{liq}$ is computed such that a certain excess air ratio is met
- excess air ratio, λ—controlled via $\dot{m}_{liq}$
- turbine inlet temperature (TIT)—controlled by the fuel mass flow to its respective input value
- pressure at the intercooler inlet, p_{IC}—specified by an input value
- working pressure, p–pressure at the CMB inlet—specified by an input value
- temperature approach between water temperature at the EVA inlet and drum temperature, $\Delta T_{EVA,out}$—specified by an input value
- steam outlet temperature of superheater, $T_{SH,out}$—degree of superheating—specified by an input value

The IC and EVA feature two operational settings for computing the steam flow rate. In the first case, the steam flow rate is defined by the user, and the heat and mass balance is computed accordingly. In the other case, steam generation is calculated based on the limiting pinch point of the heat exchangers or the available heat, respectively. The amount of steam raised in the IC then depends on the LPC back pressure (the higher the IC pressure, the more compression heat is available for steam raising). In the HRSG, the amount of steam

produced is a function of the turbine's exhaust temperature (turbine outlet temperature (TOT)), which in turn depends on the working pressure and flow rate.

As mentioned above, the water re-introduced into the cycle fully stems from exhaust condensation.

The hot flue gas is subsequently expanded in two turbines, the HPT and the LPT. The gas enters the HPT at the working pressure minus the pressure drop in the combustor and is expanded to the LPT inlet pressure (the same as the IC pressure). The expansion in the LPT decreases the pressure to near ambient pressure in two stages, which operate at an equal pressure ratio. The cooling mass flows are calculated simultaneously. The acceptable blade temperature of the HPT is set to 950 °C and to 900 °C for the LPT, respectively. Present-day turbine blade material supports operation at these specifications in uncooled machines, e.g., the microturbine system Turbec T100 [25].

4. Results and Discussion

In the following, the performance of TopCycle will be analyzed with a focus on the effect of the previously introduced parameters. After investigating the cycle's behavior towards its steam raising mechanisms, TopCycle's performance map is thoroughly studied. Finally, a sensitivity analysis investigates the impact of the control parameter on the electric efficiency.

4.1. Steam and Air Ratio Investigation

TopCycle as a humidified cycle allows a performance analysis on its fundamental characteristic, the steam ratio Ω, defined as follows:

$$\Omega = \left.\frac{\dot{m}_{steam}}{\dot{m}_{air}}\right|_{CMB} \tag{6}$$

In TopCycle, steam is raised by two different mechanisms: by heat recovery in the intercooler (IC) and in the evaporator (EVA), and further by vaporizing water (liq) directly in the combustor (CMB). The steam ratio Ω considers only the steam mass flow present in the CMB and does therefore not differentiate between the mechanisms.

In the following, the cycle will be analyzed for these steam raising mechanisms by introducing the subsequently presented cases (Table 3). The cases either cover a variation in steam flow raised by intercooling (IC) $\dot{m}_{IC}$ while keeping the water flow $\dot{m}_{liq}$ injected into the CMB constant (Cases 1, 2, 3) or vice versa (Cases 1, 4, 5). The herein presented mass flow values are input in the simulation. All other cycle parameters are fixed such as IC pressure, working pressure, and TIT. For each case, the variation of Ω is then only realized by varying the steam flow rate of the EVA $\dot{m}_{EVA}$. Here, also, $\dot{m}_{EVA}$ is controlled by the user-defined set point, which is increased with increasing Ω. In this part of the results, the excess air ratio λ is mainly a function of Ω, as can be seen by comparing Figures 3b and 4b.

Table 3. Analyzed cases.

Case	Water to CMB $\dot{m}_{liq}$ (kg/s)	Steam Raised in IC $\dot{m}_{IC}$ (kg/s)	Steam Raised in EVA $\dot{m}_{EVA}$ (kg/s)
1	0	1	3–5.5
2	0	1.5	3–5.5
3	0	2	3–5.5
4	1	1	3–5.5
5	2	1	3–5.5

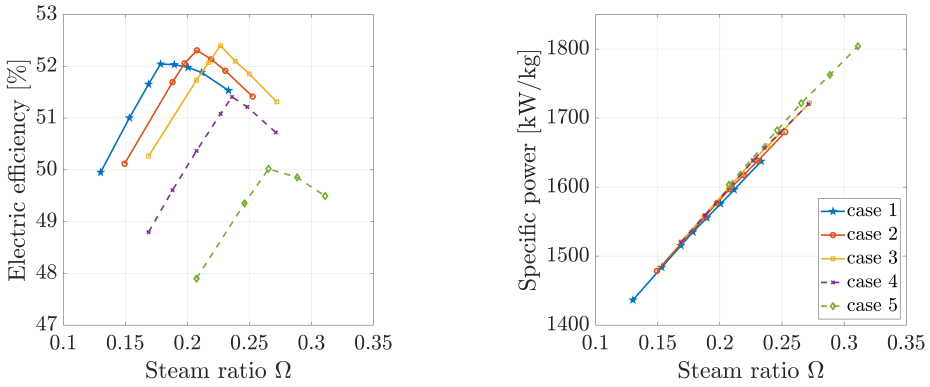

(**a**) (**b**)

Figure 3. Electric efficiency (**a**) and specific turbine power (**b**) over steam ratio Ω. The legend in (**b**) applies for both figures.

In Figure 3 the electric efficiency (a) and specific turbine power (b) are presented over Ω. The specific power is defined as the turbine power output normalized by the compressor intake mass flow (Equation (4)).

The electric efficiency shows a consistent trend for all cases. First, efficiency rises with increasing steam ratio. The more heat is recovered, the more steam is raised in the EVA, which results in an increasing electric efficiency until reaching a turning point. Until here, the steam is superheated to a constant temperature, and the pinch point of the HRSG is located at the outlet of the superheater. By further increasing the mass flow through the EVA, a constant superheating temperature can no longer be sustained. The steam temperature starts to decrease with detrimental effects on the efficiency. The pinch point of the HRSG shifts to the inlet of the evaporator. The steam ratio can then be further increased, but the superheating temperature will decrease respectively, until the maximum amount of steam raised by exhaust heat exploitation is reached at saturated steam. This phenomenon was also described for an STIG cycle in the work of Stathopoulos et al. [7].

Cases 1 to 3 present the effect of intercooling on the cycle. In Figure 3, for an increasing $\dot{m}_{IC}$, the efficiency's turning point is shifted towards higher values of Ω. The efficiency trend results from the previously explained characteristic of the EVA operation. However, when comparing equal EVA operation points, the globally computed steam ratio Ω is increased for Cases 2 and 3 due to the elevated steam production in the IC. Therefore, in these cases, the turning point is located at an elevated steam ratio.

Further, providing additional intercooling, and thus more steam in the IC, in Cases 2 and 3, increases the compressed air density and thus reduces the further compression cost of the HPC. This process is converted into increasing maximum electric efficiency from Cases 1 to 3.

The effect of increasing the water flow injected to the CMB on the electric efficiency is shown in Cases 1, 4, and 5, where $\dot{m}_{liq}$ is increased and $\dot{m}_{IC}$ is kept constant. The turning point is again shifted to higher values of Ω for the same reasons as before.

Compared to Cases 2 and 3, the compression heat is exploited to a lesser extent, which results in the air entering the CMB at higher temperatures. Establishing a constant firing temperature (TIT) can be realized by controlling the fuel flow and by providing water or steam flow to the CMB, which exerts a cooling effect. However, evaporating water directly in the CMB instead of providing steam with heat exchangers has a detrimental effect on the efficiency, since this process is associated with the relatively higher entropy gain and cooling effect. That effect leads to the decreasing electric efficiency from Cases 1 to 4 and 5 with increasing $\dot{m}_{liq}$.

By comparing Cases 3 and 4, the difference of intercooling and water injection on the electric efficiency becomes apparent. The cumulative mass flows $\dot{m}_{liq}$ and $\dot{m}_{IC}$ are equal, and the efficiency's turning point is located at a similar steam ratio; yet, providing steam

only with the IC and EVA (Case 3) results in a higher efficiency than substituting $\dot{m}_{IC}$ for $\dot{m}_{liq}$ (Case 4) for the reasons explained.

In contrast to the efficiency, the specific turbine power (Figure 3b) is nearly a linear function of the steam ratio. More steam contributes to expansion work in the turbines and to a higher power density.

Figure 4 shows again the key performance, but this time as a function of the excess air ratio λ. Raising the steam concentration in the combustion atmosphere and thus increasing Ω exerts a higher cooling effect in the combustion chamber. In this simulation, the air flow is kept constant. Consequently, increasing the fuel flow decreases the excess air ratio λ. Converging λ towards the stoichiometric condition at $\lambda = 1$ results in an increasing flame temperature [22]. Therefore, increasing Ω by increasing steam generation shifts combustion towards stoichiometric in order to keep the firing temperature (TIT) constant, as shown in Figure 4. Hence, λ is mainly a function of Ω, and the above-described measures for increasing values of Ω are directly transferable for decreasing values of λ.

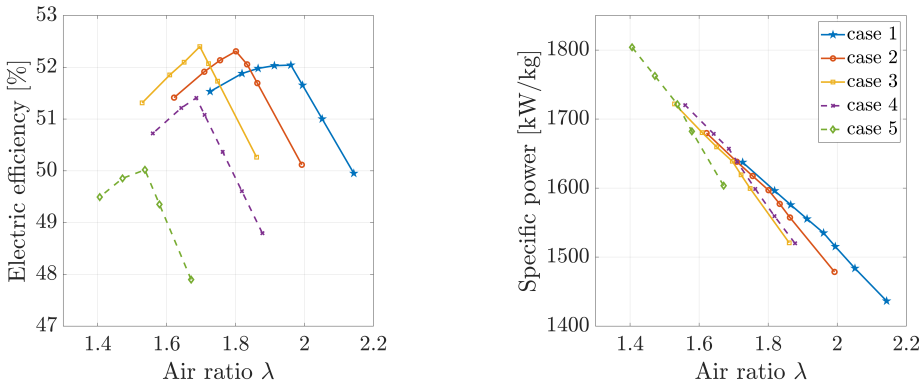

(**a**) (**b**)

Figure 4. Electrical efficiency (**a**) and turbine power (**b**) over air ratio λ. The legend in (**b**) applies for both figures.

Accordingly, the cycle can be operated within a range of parameter sets representing an optimum efficiency or power output. Increasing steam flow from the intercooler and evaporator highly benefits specific power at high efficiency, which slightly increases with increasing steam injection. Substituting steam with water leads to the same effect on the specific power, but at relatively decreased efficiency.

4.2. Investigation of TopCycle Performance Close to Stoichiometric

In the previous part of the Results Section, the cycle performance was analyzed for its steam raising mechanisms and thus for a restricted operation of the HRSG heat exchangers. In the following, the heat exchangers are specified to produce the maximum amount of steam dependent on the available heat. Further, TopCycle is operated close to the stoichiometric condition at $\lambda = 1.1$, which highly benefits the specific power.

The performance map (Figure 5) provides a useful overview of the cycle performance (electric efficiency and specific power) as a function of crucial operation parameters (working pressure and TIT). Further, the plot comprises also dependency on the IC pressure by presenting two cases for p_{IC} of 15 bar and 30 bar.

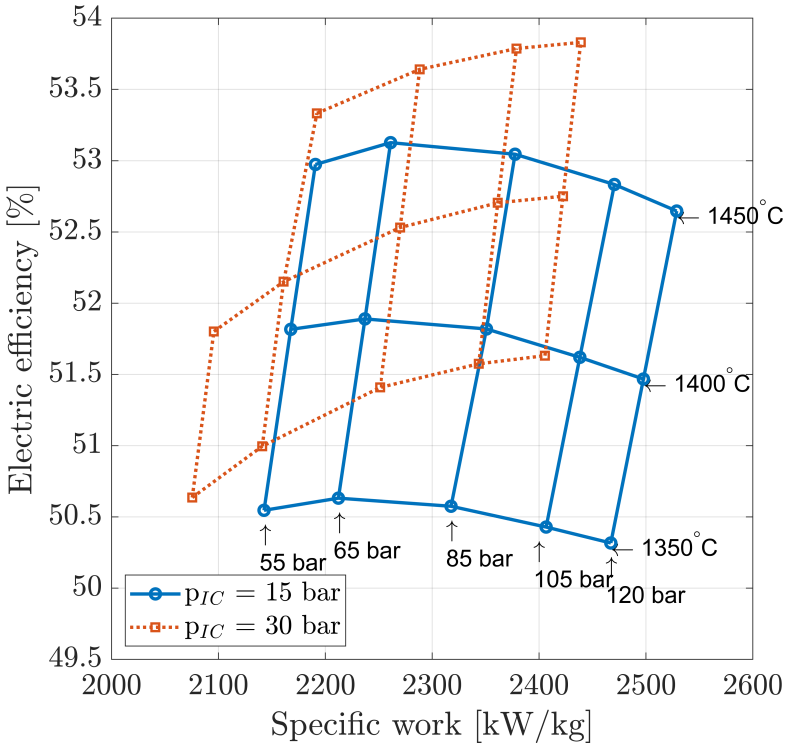

Figure 5. Performance map: electrical efficiency over specific turbine work for two cases of constant IC pressure (15 bar, blue solid lines; 30 bar, red dashed lines) and varying working pressure (vertical lines from left to right) and TIT (horizontal lines from bottom to top). Labels marking TIT and pressure apply for both cases.

In the previous section, by comparing Cases 1, 2, and 3 to Cases 1, 4, and 5, it can be seen that the gain in specific power can be realized within a broad efficiency range depending on the steam raising mechanism. Here, the cycle utilizes the maximum amount of steam production in the EVA and IC and only provides as much water as necessary to the CMB to facilitate combustion close to stoichiometric at the desired TIT.

Figure 5 displays the simulation results for two IC pressures. In both cases, increasing the TIT results in a significant rise in efficiency of over 1 percentage point per 50 K.

In humidified cycles, the water and steam injection to the CMB increases the mass flow fed to the turbines drastically, which augments the power output. At higher pressures, more work can be extracted in the turbines.

Further, the rising working pressure at constant IC pressure is realized in the HPC. Therefore, more compression heat is taken to the CMB at higher working pressures. To preserve combustion close to stoichiometric at the specified TIT, more water must be evaporated as the coolant in the CMB, which can be associated with decreasing efficiency, as shown above. The CMB allows a higher amount of water with increasing working pressure, which further benefits the specific work output.

Similar to the first part of the Results Section (Figure 3), a weak efficiency maximum can be found on the isotherms for the IC pressure p_{IC} = 15 bar. On the one hand, an optimum exists between compression costs and power generation. On the other hand, increasing the working pressure limits the steam production in the EVA, since the TOT decreases while at the same time the boiling temperature of the water increases. Both lead to a decreasing steam production in the EVA $\dot{m}_{EVA}$ at elevated working pressures. As shown in the previous section, the electric efficiency is strongly coupled to $\dot{m}_{EVA}$ and steam raising measures.

Increasing the IC pressure from 15 to 30 bar (red dashed lines), the trend of the electric efficiency indicates a maximum efficiency located outside the covered range and shifted to

higher working pressures. Increasing the IC pressure leads to higher IC inlet temperatures and thus increased intercooling duty and an elevated $\dot{m}_{IC}$. On the one hand, compressing the air to a higher level in the LPC and subsequently intercooling save compression cost in the HPC. On the other hand, increased steam production in the IC compensates decreasing steam production in the EVA with higher working pressures. As shown above, the electric efficiency is improved with rising $\dot{m}_{IC}$ (from Case 1 to 2 and 3). Thus, by increasing p_{IC}, water injected into the CMB can partly be substituted with steam from the IC for keeping TIT constant.

The efficiency trend at lower intercooling pressures resembles a CC, where an efficiency optimum can be found between the gas turbine process and heat recovery, or steam cycle, respectively. Two rather separated cycles for a CC are intertwined for humidified cycles.

4.3. Sensitivity Analysis

In the following, maximum steam production is again assumed controlled by the available heat. The effect on the cycle efficiency is determined in a sensitivity analysis. As a comparison, a base case is defined as follows:

p = 60 bar	p_{IC} = 30 bar	TIT = 1350 °C
λ = 1.1	$T_{EVA,out}$ = 20 K	$T_{SH,out}$ = 50 K.

In Figure 6a, the electric efficiency is plotted against the IC pressures for constant working pressures. For each case, an efficiency maximum can be found, marking the optimal IC pressure.

The FGC removes low temperature heat from the flue gas by condensing the steam contents therein. The total efficiency (LHV) (Figure 6b) adds the extracted heat to the useful work from the turbines. As can be seen, the total cycle works more efficiently at lower IC pressures. Lowering the IC pressure leads to an increasing temperature of the compressed air entering the combustion chamber. Hence, more water must be injected for cooling when fired at λ = 1.1. That increases the exhaust gas flow, as well as its steam content, which increases the heat extraction in the downstream FGC and hence the total cycle efficiency. A rising working pressure exerts a similar effect. Again, more compression heat is taken to the CMB with increasing pressure.

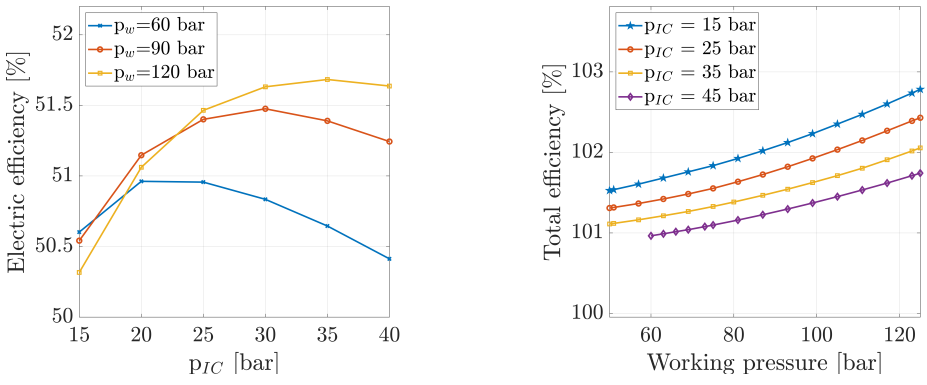

(**a**) (**b**)

Figure 6. Efficiency over the IC pressure for several working pressures (**a**) and total efficiency over working pressure for several IC pressures (**b**).

Figure 7a compares the impact on the electric efficiency of several control parameters as described in Section 3.3, while holding all other parameters constant. X is the respective percentage of the particular varied parameter, where X = 1 is the base case as defined above.

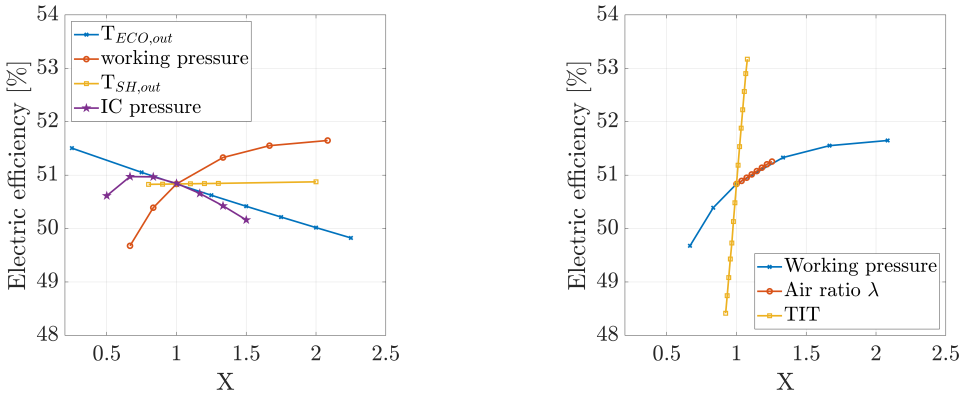

(**a**) (**b**)

Figure 7. Efficiency across the parametric study, comparing the efficiency of the economizer's water outlet temperature, working pressure, superheater's steam outlet temperature, and IC pressure (**a**) and working pressure, air ratio, and turbine inlet temperature (**b**).

The effect of the IC and working pressure on the electric efficiency is described above. A variation in IC pressure reveals a maximum in efficiency. By increasing the working pressure, the efficiency can be further maximized for higher IC pressures.

The electric efficiency also benefits from decreasing the economizer approach temperature to an operational limit. By that, more exhaust heat is recovered in the economizer, and the heat recovery cycle is optimized.

The heat recovery and with that the electric efficiency is also improved by increasing the superheating temperature. Nevertheless, utilizing more heat for superheating steam from the evaporator and intercooler leads to decreased steam production in the downstream evaporator. Consequently, this must again be compensated by increased water injection and, hence, decreased efficiency. Further, increasing steam temperatures have a detrimental effect on turbine cooling. In total, electric efficiency benefits only slightly by increased superheating temperatures. Improving heat recovery in the economizer shows a larger effect on the cycle efficiency, since here, the majority of cycle heat recovery takes place, while in the superheater, only the steam is heated.

Figure 7b presents the effect on the efficiency caused by a variation of the excess air ratio λ and TIT next to that of the working pressure as in (a), where X = 1 is again the base case. As shown in the introductory study, adding extra water or steam to the CMB is equivalent to reducing λ at constant TIT. Less water must be injected into the CMB to realize the desired TIT, and the efficiency improves.

Summarizing, the firing temperature (TIT) has the largest impact on the cycle efficiency, followed by working pressure and heat recovery, respectively. The latter is realized most effectively by optimizing the economizer performance. Increasing the excess air ratio yields a higher electric efficiency, but as shown above, this has a detrimental effect on the power density.

5. Comparison to CC

5.1. Combined Cycle Structure

TopCycle is now compared to a reference combined gas and steam turbine cycle (CC) at a similar gas turbine power output. A representative dual pressure CC integrating an SGT600 gas turbine from Siemens with supplementary firing is taken from the internal Ebsilon GTLib library containing assessed models of vendor machines [18]. Table 4 displays technical and OEMdata on the SGT600 [26]. In the simulated steam cycle, steam temperatures up to 595 °C (547 °C gas turbine (GT) exhaust) are used. Further, live steam pressure at 48 bar and condenser working pressure at 0.04 bar are assumed.

5.2. Combined Cycle TIT

The reference gas turbine SGT600 is simulated with the pre-defined model assembly provided by Ebsilon. It does not reveal results on internal gas turbine aggregate features such as TIT and the pressure ratio. One way of comparing gas turbine cycles is for identical TIT [27]. Therefore, a simple gas turbine cycle (GTC) model is created in Ebsilon, as shown in Figure 2, to identify the TIT of the SGT600.

The Siemens SGT600 consists of an axial compressor with 10 stages. After heat input, the exhaust gas is expanded in a two-stage turbine on the generator shaft and subsequently in a two-stage uncooled power turbine [28].

Table 4. Model assumptions for identifying the TIT of the SGT600 (left) and OEM SGT600 data (right).

Atmospheric pressure	(bar)	1.013	Power generation	(MW)	24.5
Pressure ratio		14:1	Gross efficiency	(%)	33.6
Compressor efficiency	(%)	85	Exhaust temperature	(°C)	543
Combustor pressure drop	(%)	3	Exhaust mass flow	(kg/s)	81.3
Turbine isentropic efficiency	(%)	88	Pressure ratio		14:1
Generator efficiency	(%)	98.5	Turbine stages		4
Mechanical efficiency	(%)	99	Cooled turbine stages		2
Acceptable blade temperature	(°C)	800			

In the following, the configuration of the GTC model used to identify the TIT of the SGT600 is introduced. Air is compressed from atmospheric conditions at the pressure ratio of the SGT600. The hot gas is expanded in two turbine stages at identical pressure ratios, where the first is cooled with compressor air. Cooling air is diverted from the compressor outlet and guided to the expander for the cooling of the vanes and blades of the first turbine stage. A large part of the compressed air is fed to the combustor. The fuel is natural gas, as defined in Table 1. A pressure drop in the combustor is assumed. The cooling of the stator and rotor is modeled according to the method described in Section 3.1. The model assumptions are presented in Table 4.

Table 5 compares the results of the GTC model with the OEM data of the SGT600 single cycle operation mode [26]. Power output, TOT, and pressure ratio are obtained from the OEM data for the simple cycle and serve as the input to the GTC model. Exhaust flow and net electrical efficiency are the output of the simulated GTC model and can again be compared to the OEM data.

The GTC model shows small relative errors to the OEM data for efficiency and exhaust flow at the respective TOT, pressure ratio, and power output. In the GTC model, TIT is further a function of the model assumptions, e.g., cooling parameters such as the acceptable blade temperature or component parameters such as the turbine efficiency.

In the next step, the GTC model is used to estimate the TIT of the SGT600 CC assembly. Therefore, the power output, TOT, and pressure ratio obtained from the Ebsilon model of the CC assembly serve as input to the GTC model, and the exhaust flow is used as the comparative parameter. As a result, for matching TOT and power output, the GTC model overestimates the exhaust mass flow compared to the CC assembly. Despite that deviation, the resulting TIT of 1152 °C will be used in the following cycle comparison between the reference CC integrating the SGT600 and TopCycle.

Table 5. Comparison of the computation to manufacturer data on the SGT600; input parameters are marked with ** and output parameters with †.

	Unit	OEMData Simple Cycle	Calculation	CC Simulation Data	Calculation
Exhaust flow †	(kg/s)	81.3	80.6	78.3	73.4
Net electric production **	(MW)	24.5	24.5	23.16	23.16
Pressure ratio **		14:1	14:1	15:1	15:1
Net electrical efficiency †	(%)	33.6	33.4	-	34.0
TOT **	(°C)	543	543	546	546
TIT †	(°C)	-	1129	-	1152

5.3. Comparison Results of the reference CC and TopCycle

The gas turbine in the reference CC simulation model produces an electrical output power of 23.2 MW, while the steam turbine adds 13.9 MW of electrical output power. In CC operation mode, the gas turbine's TOT is 546 °C (and TIT is estimated at 1152 °C as described above, which serves as the comparative TIT). The results of the comparison between CC and TopCycle are listed in Table 6.

In the simulation, the reference CC reaches an efficiency of 48.6% (LHV) at full load. As shown in [8], the efficiency maximum of CC is found at working pressures below 30 bar, while humidified cycles generally need higher pressures to reach their full potential. The TopCycle operated at the comparison TIT yields an electric efficiency of 45.6 % using the base case parameters specified in Section 4.1. However, when operated at design parameters (TIT of 1350 °C), TopCycle's electric efficiency is increased to levels above that of the reference CC at a similar gas turbine electric power output.

Comparing the cycles by means of specific work reveals significant differences. A minor modification of the specific work definition is done in this section, where electric output (available information) is used instead of turbine shaft power (missing information). At equal TIT conditions, TopCycle's specific power output is about four times that of the CC, when only the GT generator power is compared. Considering CC's cumulative power (GT and steam cycle generator power), TopCycle's specific work still ranks over 2.5 times higher. Consequently, TopCycle can realize a comparable electric power at a considerably smaller physical size or footprint and thus very likely investment costs.

Table 6. Comparison of reference CC and TopCycle at equal TIT and the base case. GT, gas turbine.

Parameter	Unit	Reference CC	TopCycle at TIT = 1152 °C	TopCycle Design Case
Net electric efficiency	(%)	48.6	45.6	50.8
GT electric power output	(MW)	23.2	32.0	34.4
GT specific power	(kJ/kg)	301	1260	1354
Total cycle electric power output	(MW)	37.0	32.0	34.4
Total cycle specific power	(kJ/kg)	481	1260	1354
Net cycle efficiency (incl.bleed-off)	(%)	44.4	45.6	50.8
Total cycle efficiency (incl. bleed-off)	(%)	88.9	102.5	101.3

TopCycle's exhaust heat is partially used to preheat the water fed to the combustion chamber, where in the CC, the exhaust heat is exploited entirely for steam generation. Furthermore, the HRSG of TopCycle is a single pressure type, whereas the CC uses two pressure stages. Both factors may lead to a somewhat lower efficiency of TopCycle's simulated steam part compared to that of the CC at equal TIT.

In the following, the cycles are compared for their total efficiency. After the HRSG, TopCycle's exhaust gas temperature is 106 °C. Via subsequent condensation, low tempera-

ture heat is exploited from the flue gas in the FGC, e.g., serving district heating applications. This heat contributes to the total cycle efficiency (Equation (3)).

The CC releases the stack gas at a much higher temperature of 178 °C. One way of increasing the operative flexibility of CC is realized via partial steam bleed-off from the low-pressure stage of the steam turbine and subsequent condensation [29]. Similar to TopCycle, the so extracted heat can be utilized in district heating applications.

This modification was appended to the CC model for the purpose of comparing the cycles for their total efficiency. The best results in terms of the CC's total and net electrical efficiency were achieved for the configuration described as follows (Figure 8). The combined cycle was extended by a district heating condenser (DH COND) located in the steam cycle and an additional flue gas economizer (DH ECO) downstream of the HRSG. Water was employed as the district heating (DH) medium at similar conditions as present in TopCycle at Point 3a. The DH water was heated first in the condenser and subsequently (3b) in the flue gas economizer to the desired DH supply temperature (3c). The entire steam flow was bled-off before the final steam turbine (ST) stage at Point 2a and led through the DH condenser. All simulation data are summarized in Table 7.

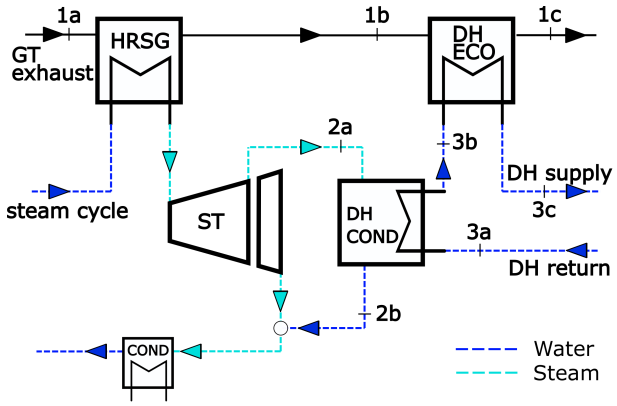

Figure 8. Schematic of the steam bleed-off section in the combined cycle. ST, steam turbine; COND, condenser.

Table 7. Model assumptions for the CC district heating addition.

DH return temperature	(°C)	40
DH supply temperature	(°C)	80
DH pressure	(bar)	8
bleed-off steam pressure	(bar)	0.5
bleed-off steam temperature	(°C)	81.3
Approach temperature condenser/economizer	(K)	8

Under these assumptions, the CC yields a total efficiency of 88.9% (LHV), while the net electrical efficiency decreases to 44.4% (LHV). In direct comparison, TopCycle operates under base case conditions at an elevated total (101.% LHV), as well as a net electrical (50.8% LHV) efficiency (Table 6).

6. Conclusions

This work introduces an innovative version of a humidified gas turbine cycle, namely TopCycle, the concept of which includes the necessary combustion infrastructure to generate highly efficient power and heat on a large variety of fuels.

TopCycle is analyzed on the basis of its fundamental feature, the steam or water admixture after compression, and for its various steam raising mechanisms. The electric efficiency benefits to some extent from exploiting compression and exhaust heat, while evaporating water directly in the combustion chamber shows penalizing effects. The study reveals a nearly linear growth of the power output with increasing steam admixture,

which is unaffected by the steam raising mechanism. By the same means, increasing the steam admixture enables combustion closer to the stoichiometric condition at the desired TIT. The steam production can be balanced such that the combustion is realized close to stoichiometric at reasonable TIT and hence enables a highly elevated power density. Also, a high total efficiency can be achieved thanks to the high dew point in the flue gas condenser at only slightly reduced electric efficiency compared to leaner combustion.

Operated at its design parameters as defined in this work and close to stoichiometric, TopCycle offers a high electric efficiency (50.8% (LHV)) and power density (over 2100 kW/kg_{air}) at a cogeneration plant size of 66 MW, where electric power output is 34 MW. Electric efficiency is at a comparable level to that of the reference CC of similar electric power output (48.6% LHV), however the power density is considerably higher in TopCycle (2.5 times that of the CC).

Hence, an equivalent power output can be realized in TopCycle at a significantly smaller plant size and thus investment costs.

A sensitivity study originating from the design case reveals the effect on TopCycle's performance exerted by selected operation parameters. Increasing TIT shows the strongest effect on the electric efficiency, which is elevated by 1 percentage point for every 50K. A similar efficiency rise can be realized by increasing the working pressure by 100% and optimizing the heat recovery by reducing the temperature approach in the economizer by 50%. Considering heat exploitation for district heating purposes, the total efficiency of the cycle is 101.3% (LHV) due to the high steam loading and hence dew point. TopCycle can thereby utilize the heat of condensation from both the steam injected in the process and from a part of the steam formed during combustion. The total efficiency can be further improved with higher working pressures and lower intercooling pressures. Modifying the CC such that steam bleed-off from the low pressure part of the steam turbine can be utilized in DH applications increases the CC's total efficiency to 88.9%, while reducing its net electrical efficiency to 44.4%. This illustrates the coexistence of high total, as well as net electrical efficiency in TopCycle.

Author Contributions: M.B. and J.P. developed the TopCycle version in its here presented form. J.P. created large parts of the TopCycle Ebsilon simulation model. S.D. modified the Ebsilon simulation model, carried out large parts of the TopCycle as well as CC simulation and analysis and wrote manuscript. All authors contributed to the conceptualization, analysis and editing. Supervised by P.S. All authors have read and agreed to the published version of the manuscript.

Funding: Swedish Energy Agency (Project number 45487-3), Phoenix Biopower.

Institutional Review Board Statement: Not applicable.

Informed Consent Statement: Not applicable.

Data Availability Statement: Data sharing not applicable.

Conflicts of Interest: The authors declare no conflict of interest.

Abbreviations

CC	Combined cycle
CHP	Combined heat and power
CT	Cooled turbine stage
DH	District heating
EvGT	Evaporative gas turbine
GT	Gas turbine
HAT	Humidified air turbine
LHV	Lower heating value
mGT	Micro gas turbine

STIG	Steam injected gas turbine
TIT	Turbine inlet temperature
TOT	Turbine outlet temperature
UCT	Uncooled turbine stage

Cycle parts

CMB	Combustor
DE	Deaerator
ECO	Economizer
EVA	Evaporator
FGC	Flue gas cooler
G	Generator
HPC	High pressure compressor
HPT	High pressure turbine
HRSG	Heat recovery steam generator
IC	Intercooler
LPC	Low pressure compressor
LPT	Low pressure turbine
SH	Superheater

Physic

$\dot{m}$	Mass flow
η	Efficiency
λ	Air ratio
Ω	Steam ratio
Ψ	Ratio of coolant and gas mass flow
m	Mass
P	Power
p	Pressure
Q	Heat
T	Temperature

References

1. Jonsson, M.; Yan, J. Humidified gas turbines—A review of proposed and implemented cycles. *Energy* **2005**, *30*, 1013–1078. [CrossRef]
2. Jonsson, M. Advanced Power Cycles with Mixtures as the Working Fluid. Ph.D. Thesis, Royal Institute of Technology, Stockholm, Sweden, 2003.
3. Traverso, A.; Massardo, A. Thermoeconomic analysis of mixed gas–steam cycles. *Appl. Therm. Eng.* **2002**, *22*, 1–21. [CrossRef]
4. Gasparovich, N.; Hellemans, J. Gas turbines with heat exchanger and water injection in the compressed air. *Proc. Instn. Mech. Engnrs.* **1971**, *185*, 953–961. [CrossRef]
5. Parente, J.; Traverso, A.; Massardo, A. Micro Humid Air Cycle: Part A—Thermodynamic and Technical Aspects. In Proceedings of the ASME Turbo Expo 2003, collocated with the 2003 International Joint Power Generation Conference, Atlanta, GA, USA, 16–19 June 2003; Volume 3. [CrossRef]
6. Parente, J.; Traverso, A.; Massardo, A. Micro Humid Air Cycle: Part B—Thermoeconomic Analysis. In Proceedings of the ASME Turbo Expo 2003, Collocated with the 2003 International Joint Power Generation Conference, Atlanta, GA, USA, 16–19 June 2003; Volume 3. [CrossRef]
7. Stathopoulos, P.; Terhaar, S.; Schimek, S.; Paschereit, C. The Ultra-Wet Cycle for High Efficiency, Low Emission Gas Turbines. In Proceedings of the Future of Gas Turbine Technology 7th International Gas Turbine Conference, Brussels, Belgium, 14–15 October 2014.
8. Bartlett, M.; Westermark, M. An Evaluation of The Thermodynamic Potential of High-Pressure Part-Flow Evaporative Gas Turbine Cycles. In Proceedings of the 17th International Conference on Efficiency, Costs, Optimization, Simulation and Environmental Impact of Energy and Process Systems, Guanajuato, Mexico, 7–9 July 2004.
9. Stathopoulos, P.; Kuhn, P.; Wendler, J.; Tanneberger, T.; Terhaar, S.; Paschereit, C.O.; Schmalhofer, C.; Griebel, P.; Aigner, M. Emissions of a wet premixed flame of natural gas and a mixture with hydrogen at high pressure. *J. Eng. Gas Turbines Power* **2016**. [CrossRef]
10. Bartlett, M. Developing Humidified Gas Turbine Cycles. Ph.D. Thesis, Royal Institute of Technology, Stockholm, Sweden, December 2002.

11. Stathopoulos, P.; Paschereit, C.O. Operational Strategies of Wet Cycle Micro Gas Turbines and Their Economic Evaluation. In Proceedings of the ASME Turbo Expo 2015: Power for Land, Sea and Air, Montreal, QC, Canada, 15–19 June 2015; p. V003T20A003. [CrossRef]
12. Stathopoulos, P.; Paschereit, C. Retrofitting micro gas turbines for wet operation. A way to increase operational flexibility in distributed CHP plants. *Appl. Energy* **2015**, *154*, 438–446. [CrossRef]
13. De Paepe, W.; Montero Carrero, M.; Bram, S.; Parente, A.; Contino, F. Toward Higher Micro Gas Turbine Efficiency and Flexibility—Humidified Micro Gas Turbines: A Review. *J. Eng. Gas Turbines Power* **2018**, *140*, 081702. [CrossRef]
14. Montero Carrero, M.; De Paepe, W.; Bram, S.; Musin, F.; Parente, A.; Contino, F. Humidified micro gas turbines for domestic users: An economic and primary energy savings analysis. *Energy* **2016**, *117*, 429–438. [CrossRef]
15. Bartlett, M.; Westermark, M. A Study of Humidified Gas Turbines for Short-Term Realization in Midsized Power Generation—Part I: Nonintercooled Cycle Analysis. *J. Eng. Gas Turbines -Power-Trans. ASME* **2005**, *127*. [CrossRef]
16. Bartlett, M.; Westermark, M. A Study of Humidified Gas Turbines for Short-Term Realization in Midsized Power Generation—Part II: Intercooled Cycle Analysis and Final Economic Evaluation. *J. Eng. Gas Turbines-Power-Trans. ASME* **2005**, *127*. [CrossRef]
17. Hansson, H.E.; Westermark, M. A Method for Operation of a Gas Turbine Group. U.S. Patent 7,721,552, 25 May 2010.
18. Steag. Available online: https://www.steag-systemtechnologies.com/de/produkte/ebsilon-professional/ (accessed on 25 September 2019).
19. IAPWS. Available online: http://www.iapws.org/index.html (accessed on 25 September 2019).
20. Werner, S. District heating and cooling in Sweden. *Energy* **2017**, *126*. [CrossRef]
21. Vattenfall. Available online: https://wärme.vattenfall.de/binaries/content/assets/waermehaus/downloads_fernwarme/faktenblatt_der_warme_berlin.pdf (accessed on 23 April 2020).
22. Baehr, H.; Kabelac, S. *Thermodynamik*; Springer: Berlin/Heidelberg, Germany, 2009.
23. Razak, A. *Industrial Gas Turbine: Performance & Operability*; Woodhead Publishing: Cambridge, UK, 2007. [CrossRef]
24. Horlock, J. *Advanced Gas Turbine Cycles*; Pergamon: Oxford, UK, 2003. [CrossRef]
25. Turbec Spa. Available online: https://people.unica.it/danielecocco/files/2012/07/Microturbina_T100_Detailed_Specifications1.pdf (accessed on 23 April 2020).
26. SiemensAG. Available online: https://new.siemens.com/global/en/products/energy/power-generation/gas-turbines/sgt-600.html# (accessed on 12 May 2020).
27. Stathopoulos, P. Comprehensive Thermodynamic Analysis of the Humphrey Cycle for Gas Turbines with Pressure Gain Combustion. *Energies* **2018**, *11*, 3521. [CrossRef]
28. SiemensAG. Available online: http://www.heinkel-systeme.de/data/simple/0056/Heinkel_Gas_Turbine_SGT-800_for_Power_Generation.pdf
(accessed on 25 September 2019).
29. Pac, P.; Suzuki, Y. Exergetic Evaluation of Gas Turbine Cogeneration Systems for District Heating and Cooling. *Int. J. Energy Res.* **1998**, *21*, 209–220. [CrossRef]